X-boson cumulant approach to the periodic Anderson model

R. Franco and M. S. Figueira
Instituto de Física, C.P. 100.093, Universidade Federal Fluminense (UFF), Avenida Litorânea s/nº, 24210-340 Niterói, Rio de Janeiro, Brazil

M. E. Foglio
Instituto de Física "Gleb Wataghin," Universidade Estadual de Campinas (UNICAMP), 13083-970 Campinas, São Paulo, Brazil
(Received 24 August 2001; published 26 July 2002)

The periodic Anderson model can be studied in the limit $U=\infty$ by employing the Hubbard X operators to project out the unwanted states. We had already studied this problem by employing the cumulant expansion with the hybridization as perturbation, but the probability conservation of the local states (completeness) is not usually satisfied when partial expansions like the "chain approximation" (CHA) are employed. To rectify this situation, we modify the CHA by employing a procedure that was used in the mean-field approximation of Coleman's slave-boson method. Our technique reproduces the features of that method in its region of validity, but avoids the unwanted phase transition that appears in the same method both when $\mu \gg E_f$ at low T and for all values of the parameters at intermediate temperatures. Our method also has a dynamic character that is absent from the mean-field slave-boson method.

DOI: 10.1103/PhysRevB.66.045112 PACS number(s): 71.10.−w, 71.27.+a, 71.28.+d, 75.20.Hr

I. INTRODUCTION

The present paper deals with the periodic Anderson model (PAM) in the limit of infinite Coulomb repulsion ($U=\infty$), and we employ the Hubbard[1] X operators to write its Hamiltonian in the form[2]

$$H=\sum_{\mathbf{k},\sigma} E_{\mathbf{k},\sigma} c^{\dagger}_{\mathbf{k},\sigma} c_{\mathbf{k},\sigma} + \sum_{j,\sigma} E_{f,j\sigma} X_{j,\sigma\sigma} + \sum_{j,\sigma,\mathbf{k}} (V_{j,\mathbf{k},\sigma} X^{\dagger}_{j,0\sigma} c_{\mathbf{k},\sigma} + V^{*}_{j,\mathbf{k},\sigma} c^{\dagger}_{\mathbf{k},\sigma} X_{j,0\sigma}). \quad (1)$$

The X operators are very convenient for working with local states associated to the sites j of a lattice, and are defined in general by $X_{j,ab}=|j,a\rangle\langle j,b|$, where the set $\{|j,a\rangle\}$ is an orthonormal basis in the space of local states of interest. There are four local states in the PAM at each site j of the lattice: the vacuum state $|j,0\rangle$, the two states $|j,\sigma\rangle$ of one electron with spin component σ, and the state $|j,2\rangle$ with two local electrons. When $U\to\infty$ the state $|j,2\rangle$ is empty, and we have used the Hubbard operators to project it out from the space of local states at site j. In this subspace of interest, the identity I_j at site j should satisfy the relation

$$X_{j,00}+X_{j,\sigma\sigma}+X_{j,\bar{\sigma}\bar{\sigma}}=I_j, \quad (2)$$

where $\bar{\sigma}$ is the spin component opposite to σ, and the three $X_{j,aa}$ are the projectors into $|j,a\rangle$.

The first term in Eq. (1) is the Hamiltonian of the conduction electrons (c electrons) and the second term describes independent localized electrons (f electrons), where a simple index j is used to identify the sites. The last term is the hybridization Hamiltonian giving the interaction between the c electrons and the f electrons, and $V_{j,\mathbf{k},\sigma}=(1/\sqrt{N_s}) \times V_{\sigma}(\mathbf{k})\exp(i\mathbf{k}.\mathbf{R}_j)$, where $\mathbf{R}_j$ is the position of site j and N_s the number of sites. Note that this interaction conserves the spin component σ.

The X operators do not satisfy the usual commutation relations, and therefore the diagrammatic methods based on Wick's theorem are not applicable. One has instead the product rules

$$X_{j,ab}.X_{j,cd}=\delta_{b,c}X_{j,ad}, \quad (3)$$

as well as a diagrammatic cumulant expansion with a linked cluster theorem that was originally employed by Hubbard[1] to study his model. In the present work we shall use an extension of this expansion to the PAM,[2,3] that can be used to calculate the Green's functions (GF's), and the occupation numbers $n_{j,a}=\langle X_{j,aa}\rangle$ are then obtained from the appropriate one-electron GF. Assuming translational invariance we can write $n_{j,a}=n_a$ (independent of j), so that from Eq. (2) it follows that

$$n_0+n_{\sigma}+n_{\bar{\sigma}}=1. \quad (4)$$

We shall call this relation "completeness," and it is essential that it would be satisfied to avoid distortions in the values of physical properties calculated with those GF's. We have found that completeness is not usually satisfied when only approximate cumulant GF's (Ref. 4) are employed to calculate the n_a.

In the present work we shall consider a fairly simple subset of the one-electron diagrams of the cumulant expansion: the "chain approximation" (CHA). This approximation was first employed by Hewson,[5,6] and is the most general cumulant expansion with only second-order cumulants, as well as being Φ derivable.[7,8] This subset of diagrams seems very relevant, because in the absence of correlations (obtained by neglecting spin) it is the exact solution and transforms in a natural way into the corresponding Feynman's diagrammatic expansion.[2,9] When correlations are considered, this approximation presents two drawbacks: it does not show a Kondo resonance in the Kondo region, and it gives rather large departures from completeness [Eq. (4)] in this parameter re-

gion, while these departures are fairly small outside this region. In previous works we first recovered completeness by an *ad hoc* renormalization of the GF,[2] and we later conjectured[8] a way to achieve completeness by adding a set of diagrams to any arbitrary family. This result was verified for the CHA, although the resulting set of diagrams is not Φ derivable any more. Our attempts to obtain a Kondo resonance were not successful before, but we recently realized that a technique employed in the mean-field approximation of the slave-boson method[10,11] would give the desired results. To avoid multiple *f*-electron occupancy in this last method, the system's free energy is minimized subject to a constraint formally equivalent to our Eq. (2), and this procedure renormalizes the *f*-electron energy $E_{f,j\sigma}$ to a position close to the chemical potential μ, where the peak in the spectral density takes the place of the Kondo resonance. Our method then consists of renormalizing the *f*-electron energy $E_{f,j\sigma}$ of our Eq. (2) by minimizing the thermodynamic potential, with Eq. (1) as a constraint, and using Lagrange's method as was done in the slave-boson method. Note that we have only employed that aspect of the slave-boson treatment, and we have not split any of the *X* operators as a product of a fermion and a slave boson, but have used the CHA of the cumulant expansion. Our method then gives satisfactory results, because the results are very close to those obtained by the slave boson in the Kondo limit at low temperatures, while the method recovers those of the CHA at high *T* for all parameters. The unphysical second-order phase transitions that appear in the slave-boson approach in the Kondo region ($\mu \gg E_{f,j\sigma}=E_f$) at low *T*, and also for all parameters at intermediate temperatures *T*, are then eliminated by our treatment. Coleman[12] has observed that these phase transitions are artifacts of the theory, and the advantage of the present treatment is that those spurious phase transitions do not occur (a more detailed comparison of our method with the slave-boson technique is given in Secs. II and III C).

The PAM is one of several models of correlated electrons that has been very useful to describe important physical systems, like heavy fermions, Kondo systems, and transition metals. The fairly recent book of Hewson[13] discusses the techniques available to study these problems at the time of its publication, while the introduction of the limit of infinite spatial dimension[14] leads to the development of the dynamical mean-field theory (DMFT), that gives exact results in that limit. This powerful technique was discussed in a recent review,[15] and it can be said to be an extension of the Weiss mean-field theory, but with a frequency-dependent molecular field. This field is obtained from the self-consistent solution of an Anderson impurity in the presence of a fermionic bath, that represents the effect of the remaining sites of the system. The one-electron self-energy is frequency dependent, thus describing the local dynamics of the system, but it does not depend on the wave vector, so that the nonlocal correlations are lost in this treatment. A fairly recent extension[16,17] of the DMFT makes it possible to treat nonlocal correlations by also considering the interaction of a pair of fermions at different sites but employing a modified scaling of the interaction constants to avoid the disappearance of these terms in the limit of infinite dimension.[18] The effective-field problem requires now the solution of an Anderson impurity coupled to the fermionic bath, as well as to additional bosonic baths, that are again self-consistently determined. This extension was employed to study the competition between the local Kondo effect and the nonlocal Ruderman-Kittel-Kasuya-Yosida (RKKY) interaction,[19] as well as the related locally critical quantum phase transitions.[20,21]

Our method does not have the space dynamics characteristic of the extended DMFT, but it retains some time dynamics, although of a much simpler type than that provided by the DMFT (cf. our discussion of the *X*-boson self-energy in Appendix, Sec. 1). The *X*-boson method would then have, like the DMFT, only partial relevance[15] in the study of the competition between the Kondo effect and the magnetic interactions (like the RKKY interactions). As in the case of the usual slave-boson mean-field method, it is possible, in principle, to consider a more complete subset of diagrams to include spatial fluctuations (intersite diagrams) as well as more elaborate local fluctuations, although these calculations are rather laborious.[2,3,5]

II. *X*-BOSON CUMULANT METHOD

The present work is a modification of a preliminary version[22] that was partially inspired by the mean-field approximation of Coleman's ''slave-boson'' method.[10,11] He writes the Hubbard *X* operators as a product of ordinary bosons and fermions: $X_{j,oo}\rightarrow b_j^+ b_j, X_{j,o\sigma} \rightarrow b_j^+ f_{j,\sigma}, X_{j,\sigma o}\rightarrow f_{j,\sigma}^+ b_j$, and uses the equivalent of our Eq. (4) to avoid states with more than one electron at each site *j*. In the spirit of the mean-field approximation $b_i^+ \rightarrow \langle b_i^+ \rangle = r$, and the method of Lagrangian multipliers is then used to find the ''best'' Hamiltonian that satisfies Eq. (4). The problem is then reduced to an uncorrelated Anderson lattice with renormalized hybridization $V\rightarrow rV$ and *f* level $\epsilon_f \rightarrow \epsilon_f + \lambda$.

Our method consists of adding the product of each Eq. (2) times a Lagrange multiplier Λ_j to Eq. (1), and the new Hamiltonian generates the functional that we shall minimize employing Lagrange's method. Instead of the parameter *r* we introduce

$$R \equiv \langle X_{j,oo} \rangle, \tag{5}$$

and we call the method ''*X* boson'' because the Hubbard operator $X_{j,oo}$ has a ''Bose-like'' character,[2] but note that in our method we do not write any *X* operator as a product of ordinary Fermi or Bose operators but retain them in the original Eq. (1).

Considering Eqs. (2) and (5), and employing a constant hybridization *V*, as well as site-independent local energies $E_{f,j,\sigma}=E_{f,\sigma}$ and Lagrange parameters $\Lambda_j=\Lambda$, we obtain a new Hamiltonian with the same form of Eq. (1),

$$H=\sum_{\mathbf{k},\sigma} E_{\mathbf{k},\sigma} c_{\mathbf{k},\sigma}^\dagger c_{\mathbf{k},\sigma} + \sum_{j,\sigma} \tilde{E}_{f,\sigma} X_{j,\sigma\sigma} + N_s \Lambda (R-1) + V \sum_{j,\mathbf{k},\sigma} (X_{j,0\sigma}^\dagger c_{\mathbf{k},\sigma} + c_{\mathbf{k},\sigma}^\dagger X_{j,0\sigma}), \tag{6}$$

but with a renormalized localized energy

$$\tilde{E}_{f,\sigma}=E_{f,\sigma}+\Lambda. \tag{7}$$

This procedure allows for an independent variation of R when the free energy is minimized, even though the completeness relation

$$R=1-\sum_{\sigma}\langle X_{\sigma\sigma}\rangle \tag{8}$$

must be simultaneously satisfied.

In the slave-boson approach a one-body Hamiltonian of uncorrelated particles is obtained at this stage, and Eq. (4) is then necessary to avoid the occupation of more than one localized electron per site (the conservation of probability in the space of the local states is automatically satisfied, because normal fermion operators are employed in the transformed Hamiltonian). Equation (6) on the other hand employs X operators, that force the local states to be singly occupied at most, but Eq. (4) (completeness) must be imposed here because it is not automatically satisfied when approximate GF's are employed to calculate the n_a. Although the procedure is the same as employed in the slave-boson method, the underlying physical meaning is rather different. In the present work we shall employ the GF of the chain approximation (CHA),[5,6] because it gives a fair description of the system in spite of its simplicity.

The present treatment employs the grand canonical ensemble of electrons, and instead of Eq. (1) we shall use

$$\mathcal{H}=H-\mu\left\{\sum_{\mathbf{k},\sigma} c^{\dagger}_{\mathbf{k},\sigma}c_{\mathbf{k},\sigma}+\sum_{ja}\ \nu_a X_{j,aa}\right\}, \tag{9}$$

where $\nu_a=0,1$ is the number of electrons in state $|a\rangle$. It is then convenient to define

$$\varepsilon_{j,a}=E_{f,j,a}-\mu\nu_a \tag{10}$$

and

$$\varepsilon_{\mathbf{k}\sigma}=E_{\mathbf{k}\sigma}-\mu, \tag{11}$$

because $E_{f,j,a}$ and $E_{\mathbf{k},\sigma}$ appear only in that form in all the calculations. The exact and unperturbed averages of the operator A are denoted in what follows by $\langle A\rangle_{\mathcal{H}}$ and $\langle A\rangle$, respectively.

III. THE CHAIN APPROXIMATION GREEN'S FUNCTIONS

The CHA gives simple but useful approximate propagators, obtained in the cumulant expansion by taking the infinite sum of all the diagrams that contain ionic vertices with only two lines. The laborious calculation of the general treatment[2] is rather simplified in this case, and we shall give a brief description of the technique, particularly when only the imaginary time is Fourier transformed, because this intermediate situation is not discussed in Ref. 2 and it is necessary to calculate the impurity problem. The only X_{α} and $X^{\dagger}_{\alpha}$ operators of the Fermi-type that appear in the calculation have $\alpha=(0,\sigma)$, and the f-electron GF's in real space and imaginary time are

$$G^{ff}(j,\alpha,\tau;j',\alpha',\tau')=\langle[\hat{X}_{j,\alpha}(\tau);\hat{X}^{\dagger}_{j',\alpha'}(\tau')]_{+}\rangle_{\mathcal{H}}, \tag{12}$$

where $\hat{X}_{j,\alpha}(\tau)=\exp(\tau\mathcal{H})X_{j,\alpha}\exp(-\tau\mathcal{H})$ corresponds to the Heisenberg representation and the subindex + indicates that the operators inside the parentheses are taken in the order of increasing τ to the left, with a change of sign when the two Fermi-type operators have to be exchanged to obtain this ordering.[2] In a similar way one defines the c-electron GF $G^{cc}(\mathbf{k},\sigma,\tau;\mathbf{k}',\sigma',\tau')$ as well as the mixed GF's $G^{fc}(j,\alpha,\tau;\mathbf{k}',\sigma',\tau')$ and $G^{cf}(\mathbf{k},\sigma,\tau;j',\alpha',\tau')$.

The boundary conditions of these GF with respect to τ makes possible to expand them in a Fourier series[2] employing the Matsubara frequencies $\omega_n=(2n+1)i\pi/\beta$, where n is any integer. Because of the invariance of $\mathcal{H}$ against τ translations we have frequency conservation,[2] so that $G^{ff}(j,\alpha,i\omega_n;j',\alpha',i\omega_n')=0$ unless $\omega_n+\omega_n'=0$, and one can then write

$$G^{ff}(j,\alpha,i\omega_n;j',\alpha',i\omega_n')=G^{ff}_{j\alpha;j'\alpha'}(z_n)\ \Delta(\omega_n+\omega_n') \tag{13}$$

and similar relations for the G^{cc}, G^{fc}, and G^{cf}. Here we have used $z_n\equiv i\omega_n$, and we shall keep this notation in what follows, as well as employ $\Delta(\gamma)\equiv\delta_{\gamma,0}$ (a modified notation for Kronecker's delta). The "bare GF's" (i.e., with all $V_{j,\mathbf{k},\sigma}=0$) take a fairly simple form because many of the relevant operators become statistically independent, and we then have

$$G^{ff}(j,\alpha,z_n;j',\alpha',z_n')\Rightarrow G^{0}_{f,\alpha}(z_n)\Delta(\omega_n+\omega_n')\,\delta_{j,j'}\delta_{\alpha,\alpha'}, \tag{14}$$

$$G^{cc}(\mathbf{k},\alpha,z_n;\mathbf{k}',\alpha',z_n')\Rightarrow G^{0}_{c,\mathbf{k}\sigma}(z_n)\Delta(\omega_n+\omega_n')\,\delta_{\mathbf{k},\mathbf{k}'}\delta_{\sigma,\sigma'}, \tag{15}$$

$$G^{fc}\Rightarrow G^{cf}\Rightarrow 0. \tag{16}$$

The $\delta_{\alpha,\alpha'}$ in the bare GF follows from the commutation of $\mathcal{H}$ with the z component of the spin.

The diagrams in real space that contribute to the CHA are schematized in Fig 1. The meaning of the symbols in the cumulant diagrams is the following:

(a) the "vertex" $\bullet=G^{o}_{f,0\sigma}(z_n)=-D_{0\sigma}/(z_n-\varepsilon_{f,\sigma})$ is the f bare cumulant GF, where $D_{0\sigma}=\langle X_{oo}\rangle+\langle X_{\sigma\sigma}\rangle$; (b) the "vertex" $\circ=G^{o}_{c,\mathbf{k}\sigma}(z_n)=-1/(z_n-\varepsilon_{\mathbf{k}\sigma})$ is the c bare cumulant GF; (c) the lines (edges) determine an open loop with a definite direction. When the line points to the f-vertex, it is $\leftarrow=V_{j,\mathbf{k},\sigma}$, while it is $\leftarrow=V^{*}_{j,\mathbf{k},\sigma}$ when it points to the conduction vertex; (d) the cumbersome sign and symmetry factors[1,2] are rather simple in the CHA: it is only necessary to multiply the G^{fc} and the G^{cf} times a minus sign; (e) as both the ω and the σ are conserved along the open loop, what only remains is to sum over all the internal j and $\mathbf{k}$.

We then obtain [with $\alpha=(0\sigma)$]

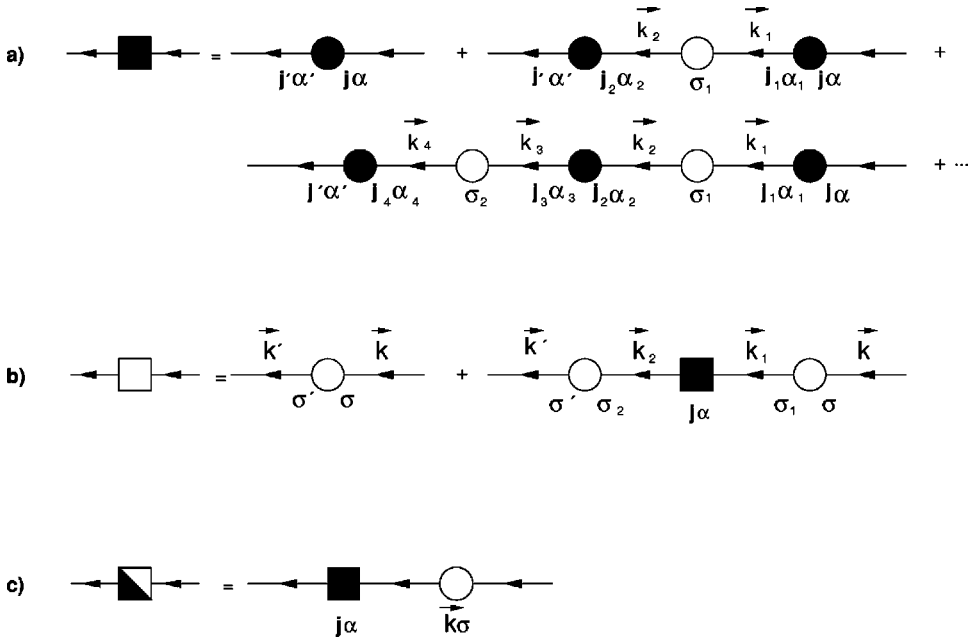

FIG. 1. The Green's-function diagrams in the CHA. The filled circles (vertices) correspond to the *f*-electron cumulants and the empty ones to those of the *c* electrons. The lines (edges) joining two vertices represent the perturbation (hybridization) (cf. Sec. III). (a) Diagrams for the *f* electron GF in the CHA. The CHA diagram for the *f* electron $G^{ff}_{j_i\alpha_i,j_f\alpha_f}(i\omega_n)$ is represented by the filled square to the left. (b) Diagrams for the *c* electron GF in the CHA. The $G^{cc}_{\mathbf{k}',\sigma';\mathbf{k},\sigma}(z_n)$ is represented by the open square symbol to the left. (c) Diagrams for the *f-c* electron GF in the CHA. The $G^{fc}_{\mathbf{j};\mathbf{k},\sigma}(z_n)$ is represented by the half filled square symbol to the left.

$$
\begin{aligned}
G^{ff}_{j'\alpha';j\alpha}(z_n) &= \delta_{\alpha',\alpha}G^o_{f,\alpha}(z_n) \\
&+ G^o_{f,\alpha}(z_n)\sum_{\mathbf{k}_1} V_{j',\mathbf{k}_1\sigma}G^o_{c,\mathbf{k}_1\sigma}(z_n)V^*_{j,\mathbf{k}_1\sigma}G^o_{f,\alpha}(z_n) \\
&+ G^o_{f,\alpha}(z_n)\sum_{\mathbf{k}_2} V_{j',\mathbf{k}_2\sigma}G^o_{c,\mathbf{k}_2\sigma}(z_n)\sum_{j_1} V^*_{j_1,\mathbf{k}_2\sigma}G^o_{f,\alpha}(z_n) \\
&\times\sum_{\mathbf{k}_1} V_{j_1,\mathbf{k}_1\sigma}G^o_{c,\mathbf{k}_1\sigma}(z_n)V^*_{j,\mathbf{k}_1\sigma}G^o_{f,\alpha}(z_n)+\ldots. \qquad (17)
\end{aligned}
$$

A. The impurity case

When there is a single impurity at a given j, each of the sums over the internal j_r reduces to a single term with $j'=j$, and we introduce

$$
\begin{aligned}
M_\sigma(z_n) &= \sum_{\mathbf{k}_1} V_{j,\mathbf{k}_1\sigma}G^o_{c,\mathbf{k}_1\sigma}(z_n)V^*_{j,\mathbf{k}_1\sigma} \\
&= \frac{1}{N_s}\sum_{\mathbf{k}} |V_\sigma(\mathbf{k})|^2 G^o_{c,\mathbf{k}\sigma}(z_n), \qquad (18)
\end{aligned}
$$

which is equal to the local GF at site j times $|V_\sigma|^2$ when the hybridization is purely local, i.e., when $V_\sigma(\mathbf{k})=V_\sigma$. Equation (17) is then a geometric series that is easily summed:

$$
\begin{aligned}
G^{ff}_{j'\alpha';j\alpha}(z_n) &= \delta_{\alpha',\alpha}\delta_{j',j}\frac{G^o_{f,\alpha}(z_n)}{1-G^o_{f,\alpha}(z_n)\ M_\sigma(z_n)} \\
&= \delta_{\alpha',\alpha}\delta_{j',j}\frac{-D_{0\sigma}}{z_n-\varepsilon_{f,\sigma}+D_{0\sigma}M_\sigma(z_n)}. \qquad (19)
\end{aligned}
$$

Employing the same technique, we obtain for the CHA the G^{cc}, that gives the scattering by the local impurity of a conduction electron $\mathbf{k},\sigma$ into $\mathbf{k}',\sigma'$:

$$
\begin{aligned}
G^{cc}_{\mathbf{k}'\sigma';\mathbf{k}\sigma}(z_n) = \delta_{\sigma',\sigma}\{&G^o_{c,\mathbf{k}\sigma}(z_n)\ \delta_{\mathbf{k},\mathbf{k}'} \\
&+ G^o_{c,\mathbf{k}'\sigma}(z_n)V^*_\sigma(\mathbf{k}')G^{ff}_{j\alpha;j\alpha}(z_n) \\
&\times V_\sigma(\mathbf{k})G^o_{c,\mathbf{k}\sigma}(z_n)\}, \qquad (20)
\end{aligned}
$$

as well as the mixed GF [with $\alpha'=(0\sigma')$],

$$
G^{fc}_{j'\boldsymbol{\alpha}';\mathbf{k}\sigma}(z_n) = \delta_{\sigma',\sigma}\delta_{j',j}G^{fc}_{j;\mathbf{k}\sigma}(z_n), \qquad (21)
$$

where we have already included the minus sign [discussed in rule (d) above] to give

$$
\begin{aligned}
G^{fc}_{j;\mathbf{k}\sigma}(z_n) &= -G^{ff}_{j\alpha;j\alpha}(z_n)V_{j,\mathbf{k}\sigma}G^o_{c,\mathbf{k}\sigma}(z_n) \\
&= -\frac{D_{0\sigma}V_{j,\mathbf{k}\sigma}}{z_n-\varepsilon_{f,\sigma}+D_{0\sigma}M_\sigma(z_n)}\times\frac{1}{z_n-\varepsilon_{\mathbf{k}\boldsymbol{\sigma}}}. \qquad (22)
\end{aligned}
$$

B. The lattice case

The case of the GF in reciprocal space and imaginary frequencies has been discussed in detail in Ref. 2 and in the CHA one follows the same prescriptions given above, but replaces the sum over internal j and $\mathbf{k}$ by a conservation of $\mathbf{k}$ along the whole chain, so that we have

$$
\begin{aligned}
&G^{ff}[\mathbf{k}',(0\sigma'),z'_n;\mathbf{k},(0\sigma),z_n] \\
&\quad = \delta_{\mathbf{k},\mathbf{k}'}\delta_{\sigma,\sigma'}\Delta(\omega_n+\omega'_n)G^{ff}_{\mathbf{k}\sigma}(z_n), \qquad (23)
\end{aligned}
$$

$$
G^{cc}(\mathbf{k}',\sigma',z'_n;\mathbf{k},\sigma,z_n) = \delta_{\mathbf{k},\mathbf{k}'}\delta_{\sigma,\sigma'}\Delta(\omega_n+\omega'_n)G^{cc}_{\mathbf{k}\sigma}(z_n), \qquad (24)
$$

$$
G^{fc}[\mathbf{k}',(0\sigma'),z'_n;\mathbf{k},\sigma,z_n] = \delta_{\mathbf{k},\mathbf{k}'}\delta_{\sigma,\sigma'}\Delta(\omega_n+\omega'_n)G^{fc}_{\mathbf{k}\sigma}(z_n), \qquad (25)
$$

where

$$G^{ff}_{\mathbf{k}\sigma}(z_n)=\frac{-D_\sigma(z_n-\varepsilon_{\mathbf{k}\sigma})}{(z_n-\varepsilon_{f,\sigma})(z_n-\varepsilon_{\mathbf{k}\sigma})-|V_\sigma(\mathbf{k})|^2D_\sigma}, \quad (26)$$

$$G^{cc}_{\mathbf{k}\sigma}(z_n)=\frac{-(z_n-\varepsilon_{f,\sigma})}{(z_n-\varepsilon_{f,\sigma})(z_n-\varepsilon_{\mathbf{k}\sigma})-|V_\sigma(\mathbf{k})|^2D_\sigma}, \quad (27)$$

and

$$G^{fc}_{\mathbf{k}\sigma}(z_n)=\frac{-D_\sigma V_\sigma(\mathbf{k})}{(z_n-\varepsilon_{f,\sigma})(z_n-\varepsilon_{\mathbf{k}\sigma})-|V_\sigma(\mathbf{k})|^2D_\sigma}. \quad (28)$$

C. The slave-boson GF vs the GF of the CHA

The slave-boson GF in the mean-field approximation (cf. Refs. 11, 13 and 23) are just the GF of the uncorrelated problem ($U=0$) but with a renormalized hybridization $V\rightarrow\overline{V}\equiv rV$ plus a condition that forces the local electron to an occupation less than or equal to one. The GF's of the CHA given above are formally very close to the uncorrelated ones, but they cannot be reduced to them by any change of scale [except for $D_\sigma=1$, when we recover the slave-boson Green's functions if we put $V\rightarrow rV=\overline{V}$ in Eqs. (19)–(22) and Eqs. (23)–(28)]. The obvious change $\sqrt{D_{0\sigma}}V\rightarrow\overline{V}$ leaves an extra factor $D_{0\sigma}$ in the $G^{ff}_{j'\alpha';j\alpha}(z_n)$ and $G^{ff}_{\mathbf{k}\sigma}(z_n)$, as well as $\sqrt{D_{0\sigma}}$ in both $G^{fc}_{\mathbf{j};\mathbf{k},\sigma}(z_n)$ and $G^{fc}_{\mathbf{k}\sigma}(z_n)$, and these factors are responsible for the correlation in this approximation, and lead to essential differences with the uncorrelated case.[23] In particular, they force the total occupation n_f of the f electron to $n_f\leqslant 1$, while in the uncorrelated case the relation $n_f\leqslant 2$ is satisfied. In the slave-boson method the imposed condition $n_f\leqslant 1$ is fulfilled by a shift in the local energy $\varepsilon_{f,\sigma}\rightarrow\tilde{\varepsilon}_{f,\sigma}\equiv\varepsilon_{f,\sigma}+\lambda$ and a reduction of the hybridization to $V\rightarrow\tilde{V}\equiv rV$. From an operational point of view, a shift in $\varepsilon_{f,\sigma}$ might not be sufficient to force $n_f\leqslant 1$ because the hybridization extends the f spectral density to the whole conduction band, and reducing V helps to satisfy this condition. By increasing the temperature T or the chemical potential μ the value $\tilde{V}=0$ is presently reached, leading to a decoupling of the two types of electrons that can be interpreted, from a more general point of view, as a change of phase related to a symmetry breaking of the mean-field Hamiltonian. Although the condition that forces completeness in the CHA is identical to that employed in the slave-boson method to force $n_f\leqslant 1$, it has a rather different origin, being only a consequence of using a reduced set of diagrams in the perturbative expansion,[8] and the departures from completeness are usually very moderate. In the formalism described in the present work, it is this essential difference between the two methods that eliminates the spurious phase transitions appearing in the slave-boson method. An alternative explanation of this different behavior is that the X-boson solution retains some time-dependent dynamics that would remove the spurious phase transitions, while the mean-field slave-boson method does not have any relevant dynamics at all (cf. the discussion at the end of the Appendix, Sec. 1).

IV. THE SINGLE IMPURITY PROBLEM

In the X-boson approach $D_\sigma=R+n_{f\sigma}$ must be calculated self-consistently through minimization with respect to the parameter R of an adequate thermodynamic potential. When the total number of electrons N_t, the temperature T, and the volume V_s are kept constant one should minimize the Helmholtz free energy, but the same minimum is obtained by employing the thermodynamic potential $\Omega=-k_BT\ln(\mathcal{Q})$ (where $\mathcal{Q}$ is the grand partition function) and keeping T, V_s, and the chemical potential μ constant (this result is easily obtained by employing standard thermodynamic techniques).

A convenient way of calculating Ω is to employ the ξ parameter integration method.[24–26] This method introduces a ξ-dependent Hamiltonian $H(\xi)=H_o+\xi H_1$ through a coupling constant ξ (with $0\leqslant\xi\leqslant 1$), where H_1 is the hybridization in our case. For each ξ there is an associated thermodynamic potential $\Omega(\xi)$ which satisfies:

$$\left(\frac{\partial\Omega}{\partial\xi}\right)_{V_s,T,\mu}=\langle H_1(\xi)\rangle_\xi, \quad (29)$$

where $\langle A\rangle_\xi$ is the ensemble average of an operator A for a system with Hamiltonian $H(\xi)$ and the given values of μ, T, and V_s. Integrating this equation gives

$$\Omega=\Omega_o+\int_0^1 d\xi\langle H_1(\xi)\rangle_\xi, \quad (30)$$

where Ω_o is the thermodynamic potential of the system with $\xi=0$. This value of ξ corresponds to a system without hybridization, and one obtains (in the absence of magnetic field $\varepsilon_{\mathbf{k}\sigma}=\varepsilon_{\mathbf{k}}$ and $\tilde{\varepsilon}_{f\sigma}=\tilde{\varepsilon}_f$)

$$\Omega_o=-\frac{2}{\beta}\sum_{\mathbf{k}}\ln[1+\exp(-\beta\varepsilon_{\mathbf{k}})]-\frac{1}{\beta}\ln[1+2\exp(-\beta\tilde{\varepsilon}_f)]+\Lambda(R-1), \quad (31)$$

and to calculate Ω in Eq. (30) we use

$$\langle H_1\rangle_\xi=2\mathrm{Re}\left[\sum_{\mathbf{k}\sigma}V^*_{j,\mathbf{k},\sigma}\langle c^\dagger_{\mathbf{k}\sigma}X_{0\sigma}\rangle_\xi\right]. \quad (32)$$

The average $\langle c^\dagger_{\mathbf{k}\sigma}X_{0\sigma}\rangle_\xi$ is obtained from the analytical continuation of the Matsubara $G^{fc}_{\mathbf{j};\mathbf{k},\sigma}(z_n,\xi)\rightarrow\overline{G}^{fc}_{\mathbf{j};\mathbf{k},\sigma}(z,\xi)$ into the complex upper and lower semiplanes, where $G^{fc}_{\mathbf{j};\mathbf{k},\sigma}(z_n,\xi)$ is the GF in Eq. (22) but for $V_{j,\mathbf{k},\sigma}\rightarrow\xi V_{j,\mathbf{k},\sigma}$. One then finds

$$\langle c^\dagger_{\mathbf{k},\sigma}X_{j,0\sigma}\rangle_\xi=\frac{i}{2\pi}\int_{-\infty}^{\infty}d\omega n_F(\omega)\{\overline{G}^{fc}_{j,\mathbf{k}\sigma}(\omega+i0;\xi)-\overline{G}^{fc}_{j,\mathbf{k}\sigma}(\omega-i0;\xi)\}, \quad (33)$$

where $n_F(x)=1/[1+\exp(\beta x)]$ is the Fermi-Dirac distribution. From Eqs. (18), (32) and (33) we then obtain

$$\langle H_1\rangle_\xi = -\frac{1}{\pi}\int_{-\infty}^{\infty} d\omega n_F(\omega) \times \sum_\sigma \mathrm{Im}\left\{\frac{\xi D_{0\sigma} M_\sigma(\omega^+)}{\omega^+ - \tilde{\varepsilon}_f + D_{0\sigma}\xi^2 M_\sigma(\omega^+)}\right\}, \quad (34)$$

where $\omega^+ = \omega + i0$. This equation has an interesting scaling property: it is equal to the corresponding expression of the uncorrelated system for the scaled parameter $\overline{V}_{j,\mathbf{k},\sigma} = \sqrt{D_{0\sigma}} V_{j,\mathbf{k},\sigma}$ (it is enough to remember that by replacing $D_{0\sigma}=1$ in the GF of the CHA one obtains the corresponding GF of the uncorrelated system). Rather than performing the ξ and ω integrations, we shall use the value of the Ω^u for the uncorrelated system with $\overline{V}_{j,\mathbf{k},\sigma} = \sqrt{D_{0\sigma}} V_{j,\mathbf{k},\sigma}$ and employ Eq. (30) to calculate $\int_0^1 d\xi \langle H_1^u(\xi)\rangle_\xi = \Omega^u - \Omega_o^u$, where

$$\Omega_o^u = \frac{-2}{\beta}\left[\sum_{\mathbf{k}} \ln[1+\exp(-\beta\varepsilon_{\mathbf{k}})] + \ln[1+\exp(-\beta\tilde{\varepsilon}_f)]\right] + \Lambda(R-1) \quad (35)$$

is the Ω^u for $\overline{V}_{j,\mathbf{k},\sigma}=0$. In our case the unperturbed Hamiltonian for the lattice problem is

$$H^u = \sum_{\mathbf{k},\sigma} \varepsilon_{\mathbf{k},\sigma} c^\dagger_{\mathbf{k},\sigma} c_{\mathbf{k},\sigma} + \sum_{j,\sigma} \tilde{\varepsilon}_f f^\dagger_{j,\sigma} f_{j,\sigma} + N_s\Lambda(R-1) + \sum_{j,\mathbf{k},\sigma} (\overline{V}_{j,\mathbf{k},\sigma} f^\dagger_{j,\sigma} c_{\mathbf{k},\sigma} + \overline{V}^*_{j,\mathbf{k},\sigma} c^\dagger_{\mathbf{k},\sigma} f_{j,\sigma}), \quad (36)$$

and in the impurity case the sum over sites reduces to the impurity site and $N_s\Lambda(R-1)\to\Lambda(R-1)$. This Hamiltonian can be easily diagonalized, and the corresponding $\mathcal{H}^u$ can be written

$$\mathcal{H}^u = \sum_{i,\sigma} \omega_{i,\sigma}\alpha^\dagger_{i,\sigma}\alpha_{i,\sigma} + \Lambda(R-1), \quad (37)$$

where $\alpha^\dagger_{i,\sigma}$ ($\alpha_{i,\sigma}$) are the creation (destruction) operators of the composite particles of energies $\omega_{i,\sigma}$ (there are N_s+1 states for each spin σ). The calculation of

$$\Omega^u = \frac{-1}{\beta}\sum_{i\sigma} \ln[1+\exp(-\beta\omega_{i,\sigma})] + \Lambda(R-1), \quad (38)$$

is straightforward, and employing Eqs. (30), (31), (35), and (38) we find

$$\Omega = \overline{\Omega}_0 + \frac{-1}{\beta}\sum_{i\sigma} \ln[1+\exp(-\beta\omega_{i,\sigma})] + \Lambda(R-1), \quad (39)$$

where

$$\overline{\Omega}_0 \equiv \Omega_o - \Omega_o^u = -\frac{1}{\beta}\ln\left[\frac{1+2\exp(-\beta\tilde{\varepsilon}_f)}{[1+\exp(-\beta\tilde{\varepsilon}_f)]^2}\right], \quad (40)$$

and the eigenvalues $\omega_{i,\sigma}$ of the $\mathcal{H}^u$ are just given by the poles of the GF in the CHA [Eq. (19)].

It is interesting that all the correlation effects on the thermodynamic potential appear in the Ω_o, that corresponds to the unperturbed system. The effect of the perturbation in the present approximation is to redistribute the energy of the quasiparticles in the same way as in an uncorrelated system with hybridization constant $\overline{V}_{j,\mathbf{k},\sigma} = \sqrt{D_{0\sigma}} V_{j,\mathbf{k},\sigma}$, and one could then expect Fermi-liquid behavior in the CHA (see a formal discussion in the Appendix).

The parameter Λ is obtained minimizing Ω with respect to R[13] (at a constant μ as discussed at the beginning of this section). To simplify the calculations we shall consider a conduction band with a constant density of states and width $W=2D$, and an hybridization constant $V_\sigma(\mathbf{k})=V$. We then obtain

$$\frac{\partial\Omega}{\partial R} = \sum_{i\sigma} n_F(\omega_{i,\sigma})\left(\frac{\partial\omega_{i,\sigma}}{\partial R}\right) + \Lambda = 0. \quad (41)$$

The poles of the impurity GF satisfy

$$\omega_{i,\sigma} = \varepsilon_f + \left(\frac{V^2 D_\sigma}{2D}\right)\ln\left[\frac{\omega_{i,\sigma}+D}{\omega_{i,\sigma}-D}\right], \quad (42)$$

and calculating the R derivative of $\omega_i(\vec{k},\sigma)$ we obtain

$$\Lambda = \frac{-V^2}{2D}\sum_{i\sigma} \ln\left(\frac{\omega_{i,\sigma}+D}{\omega_{i,\sigma}-D}\right)\frac{(\omega_{i,\sigma}^2 - D^2)n_F(\omega_{i,\sigma})}{(\omega_{i,\sigma}^2 - D^2 + V^2 D_\sigma)}. \quad (43)$$

In the absence of magnetic field, i.e., when the $\omega_{i,\sigma}=\omega_i$ is independent of σ, we can write this equation as

$$\Lambda = \frac{-V^2}{D}\int_{-\infty}^{\infty} d\omega\rho_f(\omega)\ln\left(\frac{\omega+D}{\omega-D}\right)\frac{(\omega^2-D^2)n_F(\omega)}{(\omega^2-D^2+V^2D_\sigma)}, \quad (44)$$

where $\rho_f(\omega)=\Sigma_i\delta(\omega-\omega_i)$ is the density of f states, and the chemical potential μ of the electrons was included in the single-particle energies [cf. Eqs. (10) and (11)]. The Kondo temperature

$$T_K \simeq D\exp\left(\frac{\tilde{\varepsilon}_f}{V^2}\right) \quad (45)$$

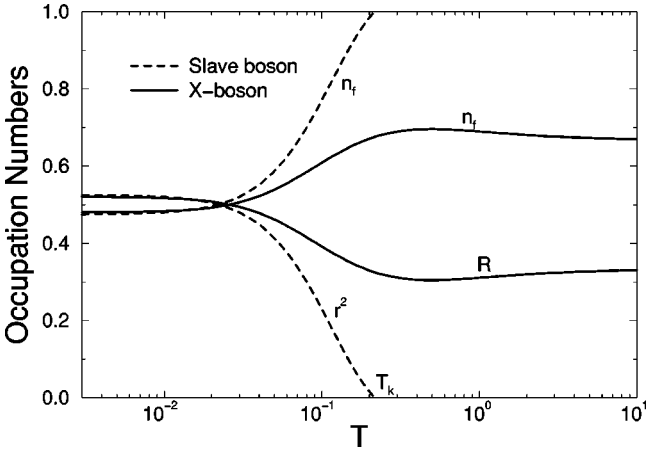

FIG. 2. Occupation numbers n_f, and parameters r^2 and R as a function of T for both the slave-boson and the X-boson methods. The figures correspond to the following parameters: $E_f=-0.15$; $W=2.0$; $V=0.3$; $\mu=0.0$.

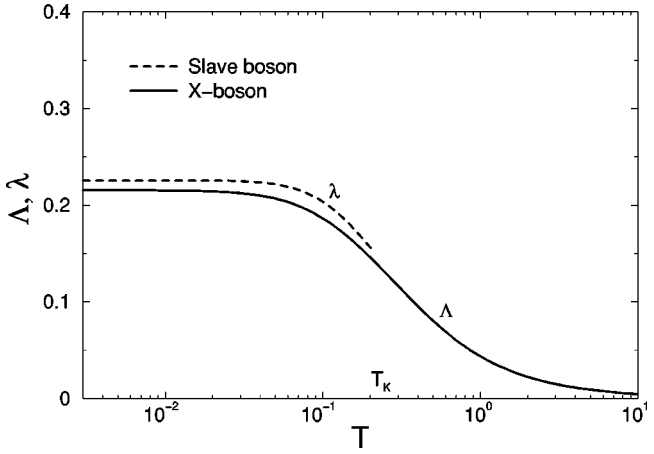

FIG. 3. Evolution with temperature T of the renormalizing Λ and λ, for the same model parameters used in Fig. 2.

is defined as the T that makes the slave-boson parameter r vanish, but another useful definition was given by Bernhard and Lacroix[27] by taking T_K as the crossover temperature, determined by the maximum of the derivative of $\langle c^{\dagger}_{i\sigma} f_{i\sigma}\rangle$ with respect to T.

V. IMPURITY RESULTS

The results presented in this section correspond to a Kondo regime with the following parameters: $Ef=-0.15$, $W=2.0$, and $V=0.3$. Figure 2 shows the evolution with T of the parameter R, that measures the hole occupation, together with the corresponding r^2 of the usual mean-field slave-boson, as well as the two occupation numbers n_f. The figure shows that $r^2 \to 0$ at a finite T (Kondo temperature T_K) while R remains positive, avoiding the spurious phase transition. The $n_f \to 1$ at T_K for the slave boson, while it remains lower than 1 for the X boson at all T.

At high temperatures the system is well described by localized moments coupled to the conduction electrons through a Coqblin-Schriefer-type Hamiltonian, and even at high temperatures there should not be a complete decoupling nor a second-order phase transition, as suggested by the mean-field slave-boson theory.[28] As the GF's of the CHA retain the correlation properties of the system, the X-boson approach shows no decoupling nor spurious phase transitions, as discussed in Sec. III C. One can see in Fig. 2 that the two approaches give similar results at low temperatures.

In Fig. 3 we represent the parameters λ and Λ as a function of temperature. We observe that the slave-boson λ breaks down at the Kondo temperature T_K whereas the X boson Λ goes continuously to zero. In the high-temperature limit the results obtained with the usual CHA are recovered by the X boson.

In Fig. 4 we show the evolution of λ, r^2, and n_f, as a function of the chemical potential μ in the usual slave-boson approach: the formalism breaks down at a value μ_0, where $n_f \to 1$. In Fig. 5 we show the evolution of the parameters Λ, R, and n_f as a function of the chemical potential μ for the X-boson approach. The results of the two approaches are similar for $\mu < \mu_0$, i.e., before the breakdown of the slave-boson method (compare Fig. 4 and Fig. 5). The parameter Λ reaches a maximum in the Kondo region and goes to zero when $\mu \gg E_f$, where $n_f \to 1$, and in this limit we recover the usual CHA.

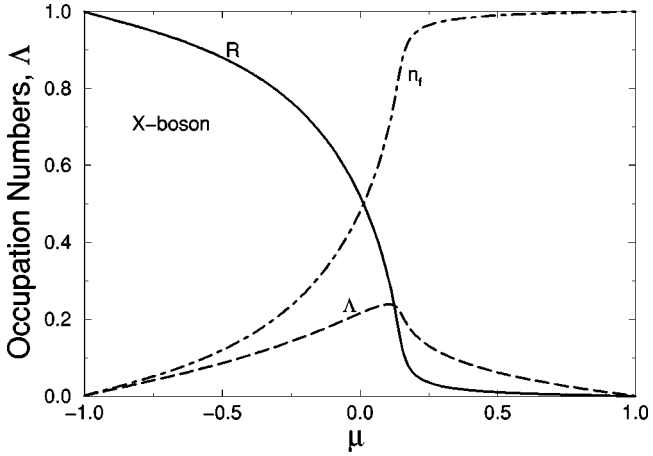

FIG. 5. X boson: Λ, R, and n_f vs μ for the same model parameters used in Fig. 4.

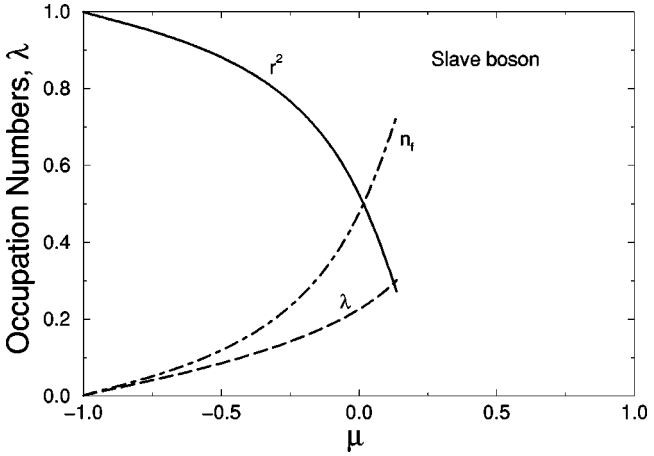

FIG. 4. Slave boson: λ, r^2, and n_f vs μ for the same model parameters used in Fig. 2 and $T=0.001$.

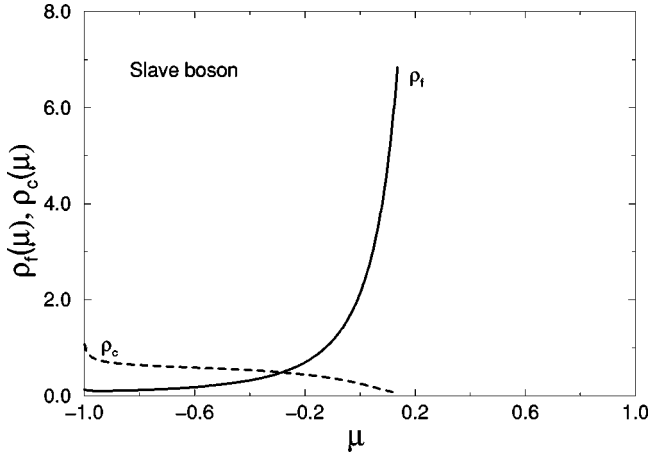

FIG. 6. Slave boson: $\rho_f(\mu), \rho_c(\mu)$ vs μ for the same model parameters used in Fig. 4.

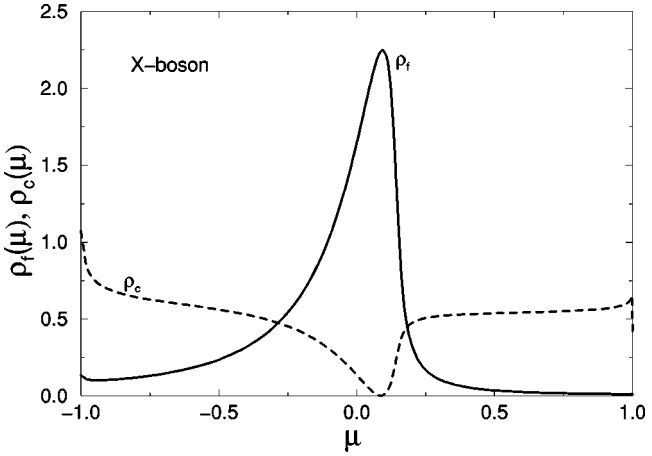

FIG. 7. X boson: $\rho_f(\mu),\rho_c(\mu)$ vs μ for the same model parameters used in Fig. 4.

The values of the f- and c-electron density of states $\rho_f(\mu)$, and $\rho_c(\mu)$ at $\omega=\mu$ are shown as a function of μ for the slave-boson method in Fig. 6 and for the X-boson approach in Fig. 7. The slave-boson plot breaks down at $\mu=\mu_0$ (where $n_f\rightarrow 1$) while for the X boson the density of states $\rho_f(\mu)$ is maximum in the Kondo region and goes to zero when $\mu \gg E_f$. In both cases one observes the transfer of conduction electrons to the f band giving rise to the Kondo resonance.

In Fig. 8 we present the density of states $\rho_f(\omega)$ and $\rho_c(\omega)$ vs energy ω in a typical Kondo situation, both for the slave-boson and X-boson treatments. The Kondo resonance appears in the two cases with a similar shape, but it is less pronounced in the X-boson treatment.

VI. THE LATTICE PROBLEM

For the lattice we follow the same technique employed with the impurity: the parameter Λ is obtained by minimizing the thermodynamic potential $\Omega=-k_BT\ln(\mathcal{Q})$ with respect to R, and $D_\sigma=R+n_{f\sigma}$ is calculated self-consistently.

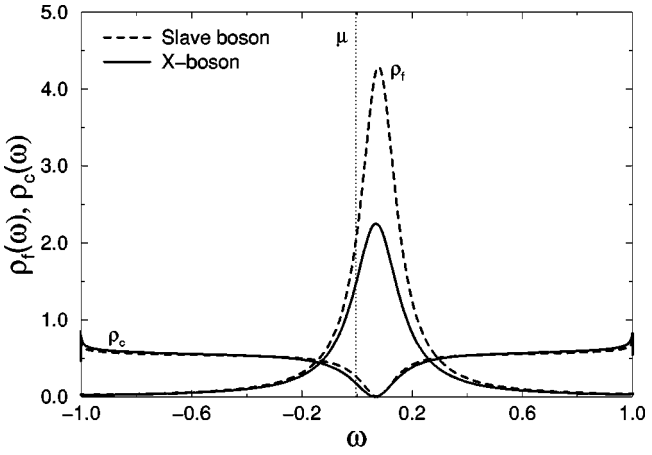

FIG. 8. Density of states of $\rho_f(\omega),\rho_c(\omega)$ vs ω in a typical Kondo situation, in the two approaches, for the same model parameters used in Fig. 4 and $\mu=0.0$.

The Ω is again obtained from Eq. (30) with adequate values of Ω_0 and $\langle H_1(\xi)\rangle_\xi$:

$$\Omega_o=-\frac{2}{\beta}\sum_{\mathbf{k}}\ln[1+\exp(-\beta\varepsilon_{\mathbf{k}})]-\frac{N_s}{\beta}\ln[1+2\exp(-\beta\tilde{\varepsilon}_f)]+N_s\Lambda(R-1), \tag{46}$$

$$\langle H_1\rangle_\xi=\frac{1}{\pi}\int_{-\infty}^{\infty}d\omega n_F(\omega)\times\sum_{\mathbf{k},\sigma}\mathrm{Im}\left\{\frac{\xi|V_\sigma(\mathbf{k})|^2D_\sigma}{(\omega^+-\varepsilon_{f\sigma})(\omega^+-\varepsilon_{\mathbf{k}\sigma})-\xi^2\,|V_\sigma(\mathbf{k})|^2D_\sigma}\right\}, \tag{47}$$

where $\omega^+=\omega+i0$. As in the impurity case, this expression coincides with that obtained for an uncorrelated Hamiltonian, which in this case is Eq. (36) with a scaled hybridization $\overline{V}_\sigma(\mathbf{k})=\sqrt{D_{0\sigma}}V_\sigma(\mathbf{k})$. The corresponding eigenvalues can be calculated analytically in this case, because for each spin component σ the Hamiltonian is reduced into N_s matrices 2×2. They are the poles of the lattice GF's, replacing the N_s+1 eigenvalues $\omega_{i,\sigma}$ of the impurity, and we denote them as

$$\omega_{\mathbf{k},\sigma}(\pm)=\frac{1}{2}(\varepsilon_{\mathbf{k},\sigma}+\tilde{\varepsilon}_f)\pm\frac{1}{2}\sqrt{(\varepsilon_{\mathbf{k},\sigma}-\tilde{\varepsilon}_f)^2+4|V_\sigma(\mathbf{k})|^2D_\sigma}. \tag{48}$$

Following the same arguments employed for the impurity we obtain

$$\Omega=\overline{\Omega}_0+\frac{-1}{\beta}\sum_{\mathbf{k},\sigma,l=\pm}\ln\{1+\exp[-\beta\omega_{\mathbf{k},\sigma}(l)]\}+N_s\Lambda(R-1), \tag{49}$$

where

$$\overline{\Omega}_0=-\frac{N_s}{\beta}\ln\left[\frac{1+2\exp(-\beta\tilde{\varepsilon}_f)}{[1+\exp(-\beta\tilde{\varepsilon}_f)]^2}\right]. \tag{50}$$

The same result was obtained by direct analytical integration, thus confirming the arguments employed in the derivation of Eqs. (39) and (49). A more complete analysis of the behavior of the thermodynamic potential can be found in Ref. 29. As in the impurity case, all the correlation effects on the thermodynamic potential appear in the Ω_o, and one expects again a Fermi-liquid behavior of the quasiparticles in the X-boson approximation (cf. the Appendix).

As in the impurity case we obtain an equation for Λ by minimizing Ω with respect to R:

$$\Lambda=\frac{1}{N_s}\sum_{\mathbf{k},\sigma}|V_\sigma(\mathbf{k})|^2\,\frac{n_F[\omega_{\mathbf{k},\sigma}(+)]-n_F[\omega_{\mathbf{k},\sigma}(-)]}{\sqrt{(\varepsilon_{\mathbf{k},\sigma}-\tilde{\varepsilon}_{f,\sigma})^2+4|V_\sigma(\mathbf{k})|^2D_\sigma}}, \tag{51}$$

where $n_F(x)$ is the Fermi-Dirac distribution. Employing $|V_\sigma(\mathbf{k})|=V$ as well as a conduction band of a constant density of states and width $W=2D$, we find for $\varepsilon_{\mathbf{k},\sigma}=\varepsilon_{\mathbf{k}}$

$$\Lambda=\frac{V^2}{D}\int_{-D}^{D}d\varepsilon_{\mathbf{k}}\frac{n_F[\omega_{\mathbf{k}}(+)]-n_F[\omega_{\mathbf{k}}(-)]}{\sqrt{(\varepsilon_{\mathbf{k}}-\tilde{\varepsilon}_f)^2+4V^2D_\sigma}}. \tag{52}$$

The quasiparticle properties of a heavy fermion system can be described by an effective Hamiltonian, characterized by two hybridized bands coupled by an effective hybridization matrix element $\overline{V}$.[28] In the slave-boson method

$$\overline{V}^2_{S-b}=(1-n_f)V^2, \tag{53}$$

while in the present approach we have

$$\overline{V}^2_{X-b}=D_\sigma V^2=(1-n_f/2)V^2. \tag{54}$$

The hybridization reduction factor is related to the effective probability that a c electron jumps into an f state, and when $U\to\infty$ this transition can only take place if the f level of the final site is empty. Rice and Ueda[30] argued that the effective hybridization should be

$$\overline{V}^2_{RU}=\frac{1-n_f}{1-n_f/2}V^2, \tag{55}$$

and variational calculations were performed by them[30] and by Fazekas.[31,32] These variational calculations present the same spurious phase transitions shown by the slave-boson method, because in all these treatments the reduction factor goes to zero at a critical temperature. On the other hand, the reduction factor does not vanish in the whole range of temperatures for the *X*-boson approach, and the f and c electrons do not decouple. All these approaches produce similar results at low temperatures.

VII. LATTICE RESULTS

We have employed for the lattice the same system parameters used to discuss the impurity, and a similar type of behavior is observed. The evolution of the *X*-boson parameters R and n_f are shown in Fig. 9 as a function of T, and the f and c electrons do not decouple in this treatment because the hole occupation $R>0$ in the whole range of temperatures, while the corresponding parameter r^2 of the usual slave-boson treatment vanishes at a critical temperature (Kondo temperature T_K). The two approaches yield similar results at low temperatures. The dependence with temperature of λ (slave-boson) and Λ (X boson) is presented in Fig. 10, and the slave boson λ breaks down at the Kondo temperature T_K whereas the X boson Λ goes continuously to zero, recovering the CHA behavior at high temperatures.

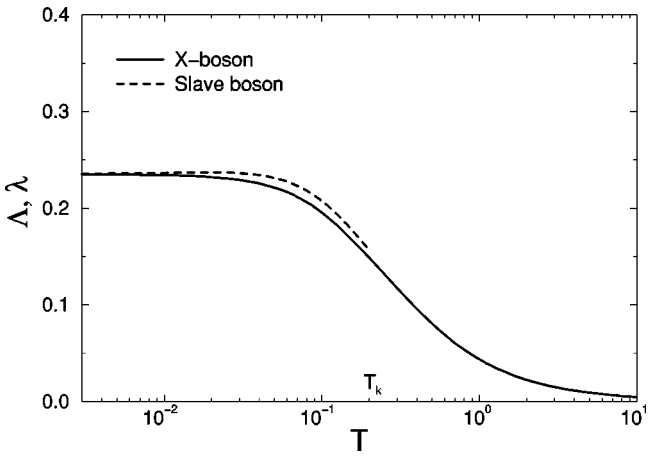

FIG. 10. Kondo case: Λ, and λ vs T for the same model parameters used in Fig. 9.

The evolution of n_f, λ, and r^2, with the chemical potential μ, is presented in Fig. 11 for the slave-boson treatment. In this case we do not recover the three characteristic regimes of the PAM: Kondo, intermediate valence, and magnetic, because the formalism breaks down when $n_f\to 1$. The corresponding quantities in the *X*-boson approach, n_f, Λ, and R, are also given as a function of μ in Fig. 12, and the three characteristic regimes of the PAM are clearly shown. There is a plateau in this figure when the chemical potential crosses the hybridization gap, and the parameter Λ is maxi-

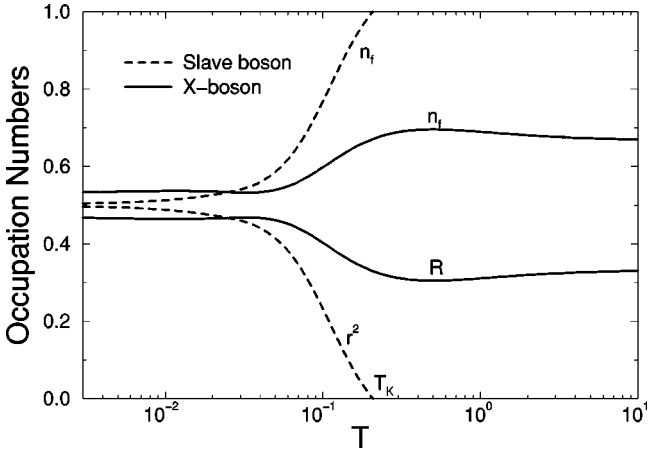

FIG. 9. Kondo case: Occupation numbers n_f, and parameters r^2 and R as a function of T for both the slave-boson and the *X*-boson methods, for the same model parameters used in Fig. 2.

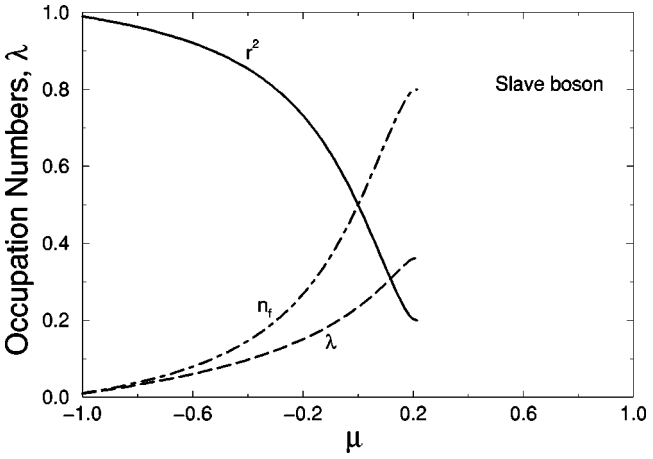

FIG. 11. slave-boson: Occupation numbers, λ, r^2, and n_f vs μ for the same model parameters used in Fig. 4.

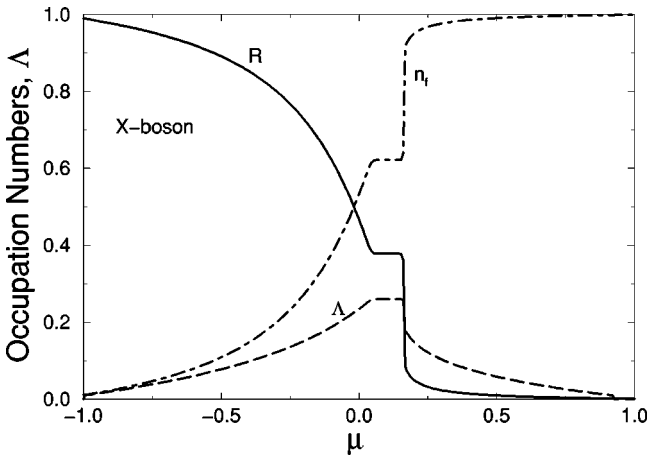

FIG. 12. *X* boson: Occupation numbers, Λ, R, and n_f vs μ for the same model parameters used in Fig. 4.

mum in the Kondo region, and goes smoothly to zero together with R when μ increases, while $n_f \rightarrow 1$. The CHA is recovered in this region by the *X*-boson treatment.

The value of the density of states $\rho_f(\mu), \rho_c(\mu)$ as function of μ is presented in Fig. 13 for the slave-boson treatment: the approach breaks down in the Kondo region when $n_f \rightarrow 1$ and the same quantities are plotted in Fig. 14 for the *X*-boson approach. The density of states $\rho_f(\omega), \rho_c(\omega)$ vs ω are shown in Fig. 15 for both the slave-boson and *X*-boson approaches in a typical Kondo situation. The density of f states at μ is practically the same in the two cases.

VIII. SPECIFIC HEAT

In this section we apply the theory developed in this work to calculate the specific heat of the Kondo insulators, but for simplicity, we shall not try to fit the experimental results of some particular compound. This class of materials has been extensively studied in the last decade since its characterization by Aeppli and Fisk[33] as Kondo insulators. Some of the compounds that we can include in this family are FeSi, $Ce_3Bi_4Pt_3$, SmB_6, and YbB_{12}. The slave boson was applied to Kondo insulators initially by Riseborough[34] and by

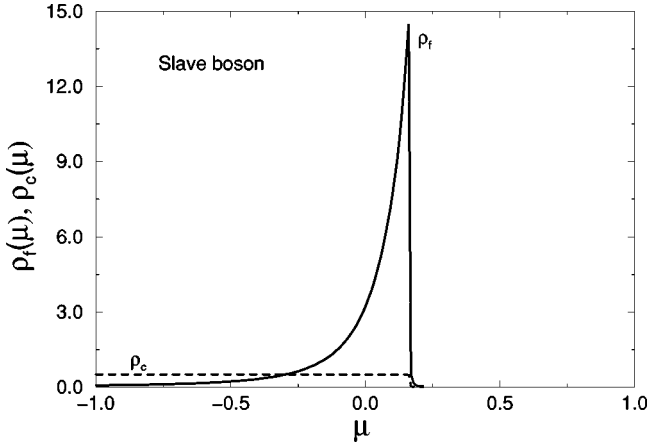

FIG. 13. Slave boson: $\rho_f(\mu), \rho_c(\mu)$ vs μ for the same model parameters used in Fig. 4.

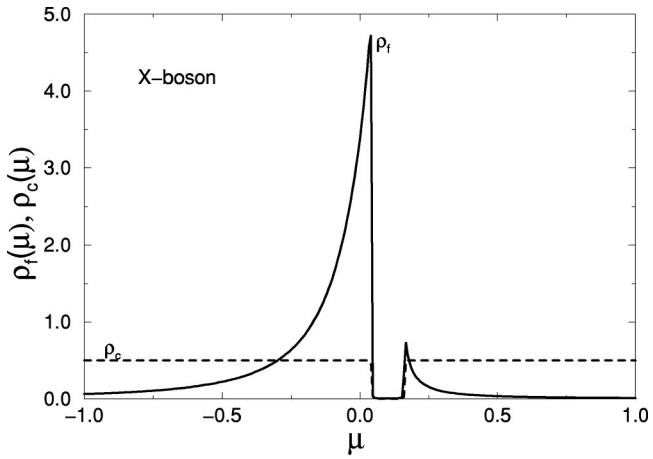

FIG. 14. *X* boson: $\rho_f(\mu), \rho_c(\mu)$ vs μ for the same model parameters used in Fig. 4.

Sanchez-Castro *et al.*,[35] and we have recently studied the Kondo insulator FeSi using the atomic model.[36,37] We have been able to adjust simultaneously the static conductivity, the resistivity, and the dynamical conductivity to the experimental results, and we obtained a fair agreement. In this section, we present the *X*-boson formalism as an alternative that gives results close to those obtained by the slave-boson method in its region of validity, while it makes it possible to extend the results to the whole range of temperatures, without presenting the spurious phase transitions appearing in the usual slave-boson method.

To calculate the specific heat employing Ω we first show by standard thermodynamic techniques that

$$S = -\left(\frac{\partial F}{\partial T}\right)_{N,V} = -\left(\frac{\partial \Omega}{\partial T}\right)_{\mu,V}, \tag{56}$$

and then that

$$C_v = T\left(\frac{\partial S}{\partial T}\right)_{N,V} = -T\left(\frac{\partial^2 \Omega}{\partial T^2}\right)_{\mu,V} + T\left(\frac{\partial \mu}{\partial T}\right)_{N,V}\left(\frac{\partial N}{\partial T}\right)_{\mu,V}. \tag{57}$$

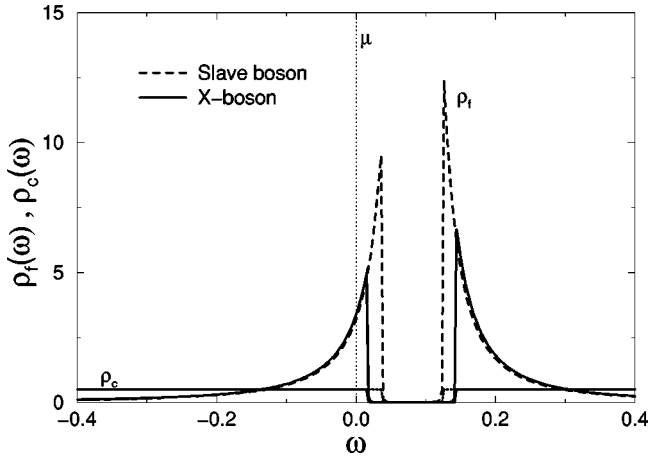

FIG. 15. Density of states in a typical Kondo situation in the two approaches: $\rho(\omega)$ vs ω for the same model parameters used in Fig. 4 and $T = 0.001$.

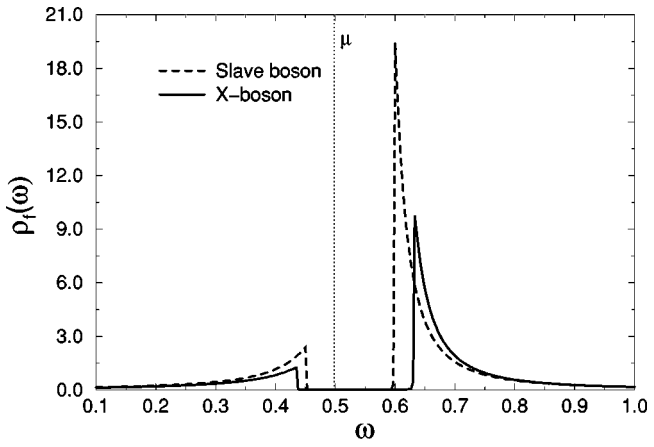

FIG. 16. Density of states in a typical Kondo insulator situation in the two approaches: $\rho_f(\omega)$ vs ω with the following parameters: $E_f=0.3$; $W=2.0$; $V=0.35$; $\mu=0.5$; $T=0.001$.

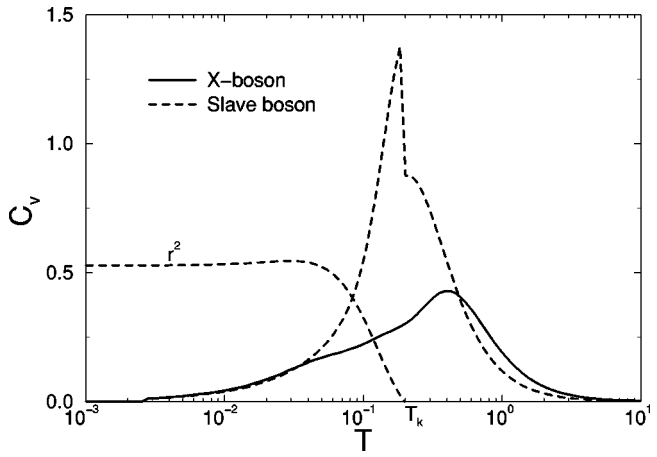

FIG. 17. Kondo insulator: Specific heat of a typical Kondo insulator for the same model parameters used in Fig. 16 but as a function of temperature.

Assuming a conduction band with a constant density of states, width $W=2D$, and the absence of magnetic field, we find from Eqs. (49) and (50) that

$$-T\left(\frac{\partial^2\Omega}{\partial T^2}\right)_{\mu,V} = -T\left(\frac{\partial^2\overline{\Omega}_0}{\partial T^2}\right)_{\mu,V} + \frac{k_B\beta^2}{D}\sum_{l=\pm}^{2}\int_{-D}^{D}dx\,\omega_l^2(x)n_F[\omega_l(x)] \times\{1-n_F[\omega_l(x)]\} - T\,N_s\left(\frac{\partial^2[\Lambda(R-1)]}{\partial T^2}\right)_{\mu,V}, \quad (58)$$

where

$$\omega_\pm(x)=\frac{1}{2}(x+\tilde{\varepsilon}_f)\pm\frac{1}{2}\sqrt{(x-\tilde{\varepsilon}_f)^2+4|V|^2D_\sigma} \quad (59)$$

and

$$-T\left(\frac{\partial^2\overline{\Omega}_0}{\partial T^2}\right)_{\mu,V} = -2N_s\,k_B\beta^2\tilde{\varepsilon}_f^2\exp(\beta\tilde{\varepsilon}_f) \times\frac{[3+2\exp(\beta\tilde{\varepsilon}_f)]}{[\exp(\beta\tilde{\varepsilon}_f)+2]^2[\exp(\beta\tilde{\varepsilon}_f)+1]^2}. \quad (60)$$

We compare the specific heat obtained by the slave-boson vs *X*-boson methods employing in the two cases the same parameters, corresponding to a typical Kondo insulator situation with the chemical potential inside the gap. In Figure 16 we present the corresponding density of states $\rho_f(\omega)$ vs ω, for the following parameters: $E_f=0.3$, $V=0.35$, $W=2.0$, $T=0.001$, and $\mu=0.5$.

In Fig. 17 we present C_v vs T, employing the same parameters of Fig. 16. We have calculated $T(\partial\mu/\partial T)_{N,V}(\partial N/\partial T)_{\mu,V}$ numerically, and its contribution to C_V is negligible for these parameters. The calculation above the Kondo temperature T_K in the slave-boson case was performed for the phase of uncoupled *f* and *c* electrons, and the specific heat presents a discontinuity at the transition T_K, but the curve obtained by the *X*-boson method is continuous.

IX. CONCLUSIONS

The slave-boson formalism[10] has been extensively used in the mean-field approximation[11,13] to study strongly correlated electron systems, because it captures the essential physics of the Kondo effect at low temperatures and its implementation in the Kondo limit is very simple. One drawback of this method is that above a temperature T_K (cf. Sec. IV) or when $\mu\gg E_f$, it develops a spurious second-order phase transition into a phase with decoupled conduction and localized electrons. In the present work we present an approach that was inspired by some of the features of the mean-field approximation of the slave-boson method, and we obtain essentially the same results at low temperatures. We keep the *X* operators[1] even at the final stages of the calculation, while two hybridized but uncorrelated bands appear in the slave-boson method at the same stage. What we employ is the CHA (chain approximation), an approximate solution that retains electronic correlations and is a subset of the infinite diagrams of the cumulant expansion of the PAM in the limit of $U\to\infty$. The CHA corresponds to the most general set of diagrams with only second-order cumulants, and has interesting properties such as being Φ derivable.[8] The advantage of our method is that it does not have the spurious phase transitions that the mean-field slave-boson method presents at higher temperatures or chemical potentials, where our procedure behaves like the CHA solution.

We have developed the *X*-boson method both for a single local impurity and for a lattice. The correlation appears in this approximation only through the presence of a constant $D_{0\sigma}$ at critical places of the corresponding GF [cf. Eqs. (19)–(28)], but it has profound effect on the system description, forcing the local electron occupation to be $n_f<1$, and eliminating the spurious phase transitions of the slave-boson

method. When $D_{0\sigma}<1$ the GF's of the X boson have a dynamic character (cf. the Appendix, Sec. 1) that is absent in the mean-field slave-boson method (that is recovered by setting $D_{0\sigma}=1$).

From the computational point of view the X-boson method is equivalent to the slave-boson technique, and the possibility of using it for all temperatures or chemical potentials μ makes it useful as the starting point to study several interesting problems: competition between the Kondo effect and RKKY interaction in heavy fermion systems,[38–40] impurity bands in Kondo insulators,[41] non-Fermi-liquid behavior in disordered systems,[42] and the Kondo effect in quantum dots.[43,44] To give an example we have considered a Kondo insulator and calculated its specific heat: the slave-boson method shows a discontinuity at T_K, while it is continuous in the X-boson method. Although it is C_p that is usually measured, the difference C_p-C_v is usually small in liquids and solids, and shows a dependence with T similar to that obtained with the X-boson method (see, for example, the C_p of FeSi measured by Jaccarino and co-workers[45]).

In conclusion, we have presented an approach that gives essentially the same results as Coleman's slave-boson treatment at low temperatures, but without the spurious phases transitions at intermediate temperatures T or large values of μ. Our method has a dynamic character that is absent from the mean-field slave-boson method, and its results approach those of the cumulant expansion in the chain approximation for large values of T or μ.

ACKNOWLEDGMENTS

We would like to acknowledge Professors Mucio A. Continentino, E. Miranda, and E. V. Anda for helpful discussions. We are also grateful to the São Paulo State Research Foundation (FAPESP) and the National Research Council (CNPq) for their financial support.

APPENDIX: SELF-ENERGIES AND FERMI-LIQUID BEHAVIOR IN THE *X*-BOSON METHOD

1. The self-energies in the *X*-boson method

To discuss the Fermi-liquid properties of the PAM in the X-boson treatment, we shall first consider the corresponding f- and c-electron self-energies $\Sigma_f(\mathbf{k},z)$ and $\Sigma_c(\mathbf{k},z)$. We shall relate these quantities to the exact GF's by the equations

$$G^{ff}_{\mathbf{k}\sigma}(z)=\frac{-1}{[z-\tilde{\varepsilon}_{f,\sigma}-\Sigma_f(\mathbf{k},z)]}, \tag{A1}$$

$$G^{cc}_{\mathbf{k}\sigma}(z)=\frac{-1}{[z-\varepsilon_{\mathbf{k},\sigma}-\Sigma_c(\mathbf{k},z)]}, \tag{A2}$$

where we employ the z with the μ already subtracted [cf. Eqs. (10) and (11)]. Introducing an effective cumulant[36,37] $M^{eff}_{2,\mathbf{k}\sigma}(z)$ it is possible to write the exact GF's,

$$G^{ff}_{\mathbf{k}\sigma}(z)=\frac{M^{eff}_{2,\mathbf{k}\sigma}(z)}{1-|V(\vec{k})|^2 G^{o}_{c,\mathbf{k}\sigma}(z)\ M^{eff}_{2,\mathbf{k}\sigma}(z)} \tag{A3}$$

and

$$G^{cc}_{\mathbf{k}\sigma}(z)=\frac{G^{o}_{c,\mathbf{k}\sigma}(z)}{1-|V(\mathbf{k})|^2 G^{o}_{c,\mathbf{k}\sigma}(z) M^{eff}_{2,\mathbf{k}\sigma}(z)}$$

$$=\frac{-1}{z-\varepsilon_{\mathbf{k}\sigma}+|V(\mathbf{k})|^2 M^{eff}_{2,\mathbf{k}\sigma}(z)}, \tag{A4}$$

where

$$G^{o}_{c,\mathbf{k}\sigma}(z)=\frac{-1}{(z-\varepsilon_{\mathbf{k}\sigma})} \tag{A5}$$

is the unperturbed GF of the c electrons. The exact self-energies defined above are then

$$\Sigma_f(\mathbf{k},z)=z-\tilde{\varepsilon}_{f,\sigma}+[M^{eff}_{2,\mathbf{k}\sigma}(z)]^{-1}-|V(\mathbf{k})|^2 G^{o}_{c,\mathbf{k}\sigma}(z) \tag{A6}$$

and

$$\Sigma_c(\mathbf{k},z)=-|V(\mathbf{k})|^2\ M^{eff}_{2,\mathbf{k}\sigma}(z), \tag{A7}$$

and to recover the CHA self-energies it is sufficient to replace[3] the effective cumulant $M^{eff}_{2,\mathbf{k}\sigma}(z)$ by the contribution of its simplest diagram, namely, the unperturbed GF of the f electrons:

$$M^{eff}_{2,\mathbf{k}\sigma}(z)\rightarrow G^{o}_{f,0\sigma}(z)=-D_{0\sigma}/(z-\tilde{\varepsilon}_{f,\sigma}). \tag{A8}$$

It is important to notice that our definition of the self-energies differs from the usual one [see, e.g., Eqs. (277) and (278) from Ref. 15]. This is because our unperturbed problem [i.e., Eq. (1) with $V_{j,\mathbf{k},\sigma}=0$] already contains the electronic correlation ($U\rightarrow\infty$) through the $X_{j,\sigma\sigma}$ operators, while the perturbative term in the cumulant expansion is the hybridization that affects the self-energies [see Eqs. (A6) and (A7)]. Taking $\Sigma_f(\mathbf{k},z)=0$ gives $G^{ff}_{\mathbf{k}\sigma}(z)\rightarrow G^{o}_{f,0\sigma}(z)$ [cf. Eq. (A8)], which still depends on the electronic correlation through the $D_{0\sigma}$ factor.

The term $|V(\mathbf{k})|^2 G^{o}_{c,\mathbf{k}\sigma}(z)$ in our Eq. (A6) does not appear in the usual self-energies,[15] because they only give the effect of the Coulomb repulsion on the two hybridized bands without correlation, as becomes apparent by putting $\Sigma_f(i\omega_n)=0$ in both Eqs. (277) and (278) of Ref. 15.

From this discussion, it seems clear that to analyze the relevant dynamics in our description of the PAM, we have first to subtract the $|V(\mathbf{k})|^2 G^{o}_{c,\mathbf{k}\sigma}(z)$ present in Eq. (A6). This term is responsible for the usual fluctuations that appear in two hybridized but uncorrelated bands, when we look at the correlations of the local f states rather than consider the Bloch extended states. Only the relevant space and time dynamics are left, when the $|V(\mathbf{k})|^2 G^{o}_{c,\mathbf{k}\sigma}(z)$ is eliminated from our exact $\Sigma_f(\mathbf{k},z)$, and then we obtain for the CHA [cf. Eq. (A8)]

$$\Sigma_{f\sigma}(\mathbf{k},z)\rightarrow z-\tilde{\varepsilon}_{f,\sigma}+[M^{eff}_{2,\mathbf{k}\sigma}(z)]^{-1}$$
$$=-(z-\tilde{\varepsilon}_{f,\sigma})\frac{1-D_{0\sigma}}{D_{0\sigma}}. \quad \text{(A9)}$$

The same arguments can be employed for $\Sigma_{c\sigma}(\mathbf{k},z)$, and one finds that the relevant self-energy for our purpose is

$$\Sigma_{c\sigma}(\mathbf{k},z)\rightarrow-|V(\vec{k})|^2\left[M^{eff}_{2,\mathbf{k}\sigma}(z)+\frac{1}{z-\tilde{\varepsilon}_{f,\sigma}}\right], \quad \text{(A10)}$$

and employing Eq. (A8) for the CHA we then find

$$\Sigma_{c\sigma}(\mathbf{k},z)\rightarrow-|V(\vec{k})|^2\frac{1-D_{0\sigma}}{z-\tilde{\varepsilon}_{f,\sigma}}. \quad \text{(A11)}$$

Equations (A9) and (A11) show that although there is no relevant spatial dependence in the self-energies of the CHA, they do retain some local time dependence. As discussed in Sec. III C, the mean-field slave-boson GF is recovered by replacing $D_{0\sigma}\rightarrow 1$, and the corresponding self-energy vanishes, showing that all the local time dependence is completely lost in the self-energies of that method. The spurious phase transition observed in the slave-boson method is absent from the *X*-boson description, and this result seems to indicate that the time dynamics retained in the CHA is able to suppress those transitions.

2. Fermi-liquid properties in the *X*-boson method

The essential property of a Fermi-liquid is that at low temperatures it has a behavior close to that of a system of free fermions. It is described by a system of quasiparticles that replace the elementary excitations of the free system, but they have a finite lifetime caused by the interactions that are absent in the free system. Instead of the elementary particle energies we have to analyze the poles of the relevant GF, given in our problem by the solutions $z_{\mathbf{k}\sigma}$ of the equation

$$z-\varepsilon_{\mathbf{k}\sigma}+|V(\mathbf{k})|^2M^{eff}_{2,\mathbf{k}\sigma}(z)=0. \quad \text{(A12)}$$

The $\mathrm{Re}[z_{\mathbf{k}\sigma}]$ corresponds to the energies of the elementary excitations, while their imaginary parts give their decay properties, and the Fermi surface is given by the set of $\mathbf{k}_F$ such that $\mathrm{Re}[z_{\mathbf{k}\sigma}]=0$, because we already subtracted the μ from the z. The $M^{eff}_{2,\mathbf{k}\sigma}(z)$ in the numerator of Eq. (A3) does not introduce new poles, because $G^{ff}_{\mathbf{k}\sigma}(z)$ is finite at those poles.

From Eq. (A12) we obtain

$$M^{eff}_{2,\mathbf{k}\sigma}(z_{\mathbf{k}\sigma})=-\frac{z_{\mathbf{k}\sigma}-\varepsilon_{\mathbf{k}\sigma}}{|V(\mathbf{k})|^2},$$

and replacing in Eq. (A6) we find

$$\Sigma_f(\mathbf{k},z_{\mathbf{k}\sigma})=z_{\mathbf{k}\sigma}-\tilde{\varepsilon}_{f,\sigma}, \quad \text{(A13)}$$

while from Eqs. (A8) and (A12) we obtain

$$\Sigma_c(\mathbf{k},z_{\mathbf{k}\sigma})=z_{\mathbf{k}\sigma}-\varepsilon_{\mathbf{k}\sigma}. \quad \text{(A14)}$$

It then follows that

$$\mathrm{Im}[\Sigma_c(\mathbf{k},z_{\mathbf{k}\sigma})]=\mathrm{Im}[\Sigma_f(\mathbf{k},z_{\mathbf{k}\sigma})]=\mathrm{Im}[z_{\mathbf{k}\sigma}]. \quad \text{(A15)}$$

An essential property of the Fermi-liquid is that the quasiparticles on the Fermi surface have an infinite lifetime when $T\rightarrow 0$, and this property follows from Eq. (A15) for both the *f* and *c* electrons when the poles on the Fermi surface are real, because the corresponding self-energies are then also real.

From Eq. (48) we conclude that the GF poles of the PAM in the CHA are all real, and the same property holds for the *X*-boson solution. These two approximations therefore describe the PAM as a Fermi-liquid, because they satisfy the condition above. Because the infinite lifetime is valid for all $\mathbf{k}$ and for all *T*, the quasiparticles in these two approximations behave more elementary excitations than like the usual quasiparticles, that have a finite lifetime outside the Fermi surface, even at $T\rightarrow 0$.

[1] J. Hubbard, Proc. R. Soc. London, Ser. A **285**, 542 (1965); **296**, 82 (1966).
[2] M.S. Figueira, M.E. Foglio, and G.G. Martinez, Phys. Rev. B **50**, 17 933 (1994).
[3] M.E. Foglio and M.S. Figueira, J. Phys. A **30**, 7879 (1997).
[4] M.E. Foglio and M.S. Figueira, Int. J. Mod. Phys. B **12**, 837 (1998).
[5] A.C. Hewson, J. Phys. C **10**, 4973 (1977).
[6] E.V. Anda, J. Phys. C **14**, L1037 (1981).
[7] G. Baym and L.P. Kadanoff, Phys. Rev. **124**, 287 (1961).
[8] M.S. Figueira and M.E. Foglio, J. Phys.: Condens. Matter **8**, 5017 (1996).
[9] G. G. Martinez Pino, Ph.D. thesis, Universidade Estadual de Campinas, 1989.
[10] P. Coleman, Phys. Rev. B **29**, 3035 (1984).
[11] D.M. Newns and N. Read, Adv. Phys. **36**, 799 (1987).
[12] P. Coleman, J. Magn. Magn. Mater. **47&48**, 323 (1985).
[13] A. C. Hewson, *The Kondo Problem to Heavy Fermions* (Cambridge University, Cambridge, England, 1993).
[14] W. Metzner and D. Vollhardt, Phys. Rev. Lett. **62**, 324 (1989).
[15] A. Georges, G. Kotliar, W. Krauth, and M.J. Rozenberg, Rev. Mod. Phys. **68**, 13 (1996).
[16] Q. Si and J.L. Smith, Phys. Rev. Lett. **77**, 3391 (1996).
[17] J.L. Smith and Q. Si, Europhys. Lett. **35**, 228 (1999).
[18] J.L. Smith and Q. Si, Phys. Rev. B **61**, 5184 (2000).
[19] S. Doniach, Physica B **91**, 231 (1977).
[20] Qimiao Si, Silvio Rabello, Kevin Ingersent, and J. Lleweilun Smith, Nature (London) **413**, 804 (2001).
[21] Mucio A. Continentino, *Quantum Scaling in Many-Body Systems*, World Scientific Lecture Notes in Physics Vol. 67 (World Scientific, Singapore, 2001).
[22] R. Franco, M.S. Figueira, and M.E. Foglio, J. Magn. Magn. Mater. **47&48**, 323 (2001).
[23] M.E. Foglio, Phys. Rev. B **43**, 3192 (1991).

[24] M.S. Figueira and M.E. Foglio, Physica A **208**, 279 (1994).
[25] A. A. Abrikosov, L. P. Gorkov, and I. E. Dzyaloshinski, *Quantum Field Theoretical Methods in Statistical Physics* (Pergamon, Oxford, 1965).
[26] S. Doniach and E. H. Sondheimer, *Green's Functions for Solid State Physicists* (Benjamin, New York, 1974).
[27] B.H. Bernhard and Claudine Lacroix, Physica B **259-261**, 227 (1999); Phys. Rev. B **60**, 12 149 (1999).
[28] Peter Fulde, Joachim Keller, and Gertrud Zwicknagl, Solid State Phys. **41**, 1 (1988).
[29] R. Franco, M. S. Figueira, and M. E. Foglio, Physica A **308/1**, 245 (2002).
[30] T.M. Rice and K. Ueda, Phys. Rev. B **34**, 6420 (1986).
[31] P. Fazekas, J. Magn. Magn. Mater. **63&64**, 545 (1987).
[32] Patrik Fazekas, *Lecture Notes on Electron Correlation and Magnetism*, Series in Modern Condensed Matter Physics Vol. 5 (World Scientific, Singapore, 1999).
[33] G. Aeppli and Z. Fisk, Comments Condens. Matter Phys. **16**, 155 (1992).
[34] Peter S. Riseborough, Phys. Rev. B **45**, 13 984 (1992).
[35] Carlos Sanchez-Castro, Kevin S. Bedell, and Bernard R. Cooper, Phys. Rev. B **47**, 6879 (1993).
[36] M.E. Foglio and M.S. Figueira, Phys. Rev. B **60**, 11 361 (1999).
[37] M.E. Foglio and M.S. Figueira, Phys. Rev. B **62**, 7882 (2000).
[38] J.R. Iglesias, C. Lacroix, and B. Coqblin, Phys. Rev. B **56**, 11 820 (1997).
[39] T.G. Rappoport, M.S. Figueira, and M.A. Continentino, Phys. Lett. A **264**, 497 (2000).
[40] A.H. Castro Neto and B.A. Jones, Phys. Rev. B **62**, 14 975 (2000).
[41] P. Schlottmann, Phys. Rev. B **46**, 998 (1992).
[42] E. Miranda, V. Dobrosavljević, and G. Kotliar, J. Phys.: Condens. Matter **8**, 9871 (1996).
[43] Luis Craco and Kicheon Kang, Phys. Rev. B **59**, 12 244 (1999).
[44] V. Ferrari, G. Chiappe, E.V. Anda, and Maria A. Davidovich, Phys. Rev. Lett. **82**, 5088 (1999).
[45] V. Jaccarino, G.K. Wertheim, J.H. Wernick, L.R. Walker, and Sigurds Arajs, Phys. Rev. B **160**, 476 (1967).